# An Optimized Bracing System for Distributed Lateral Loads

Benjamin Jacot
Master of Engineering
Massachusetts Institute of Technology, USA
bjacot@mit.edu

Dimitrios Pagonakis
Master of Engineering
Massachusetts Institute of Technology, USA
pagonakis@alum.mit.edu

Mitchell Shope
Master of Engineering
Massachusetts Institute of Technology, USA

Corentin Fivet
PhD, Prof., Structural Xploration Lab
Ecole Polytechnique Fédérale de Lausanne, Switzerland
corentin.fivet@epfl.ch

John Ochsendorf
PhD, Prof., Dept. of Arch., Dept. of CEE
Massachusetts Institute of Technology, USA

*Abstract*— **One of the most crucial components of a tall building is its lateral loading system. In this paper, we provide the development of a lateral bracing system that results in bracing material savings of up to 50% relative to a traditional X-Bracing system, as well as lighter corner columns due to the more efficient load paths of the lateral forces to the base. The solution naturally follows a linearized funicular curve, and the result provides a reasonable and replicable system from a manufacturing standpoint.**

*Keywords: structural optimization; bracing system; High-rise buildings.*

## I.    INTRODUCTION

An efficient bracing system against lateral wind loads can prove crucial on the material and cost savings of tall buildings. Research on optimizing lateral bracing systems of tall buildings through both gradient and heuristic methods can be found in [1], [2], [3], [4], [5] and [6].

In this paper, we present a new bracing typology (Figure 1) that further minimizes the static action criteria.

The assumptions related to the model are those of classical truss models: self-weight of the elements is neglected, elements only develop axial forces, weight and volume of connections are neglected, and loads act at the joints only. These restrictions are reasonable when considering the early definition of a lateral bracing system with a predominant load case. Static action [7], also known as load-path [8], is defined as:

$$\omega = \sum_{i=0}^{n} |f_i|\, l_i$$

where $f_i$ and $l_i$ are the $n$ member forces and lengths, respectively.

This criteria can be directly related to the volume and total strain energy of the structural network [8][9]. Indeed, if a constant stress $\sigma = f_i/a_i$ is assumed in every member of the network (same stress in tension and in compression), the following holds:

$$\text{volume} = \sum_{i=0}^{n} a_i l_i = \sum_{i=0}^{n} \frac{|f_i|}{\sigma} l_i = \frac{1}{\sigma}\sum_{i=0}^{n} |f_i| l_i = \frac{\omega}{\sigma}$$

where $a_i$ is the cross-sectional area of the members. If, in addition, every member has the same modulus of elasticity $E$:

$$\text{strain energy} = \sum_{i=0}^{n} \frac{f_i^2 l_i}{2E a_i} = \frac{\sigma}{2E}\sum_{i=0}^{n} |f_i| l_i = \frac{\sigma}{2E}\omega$$
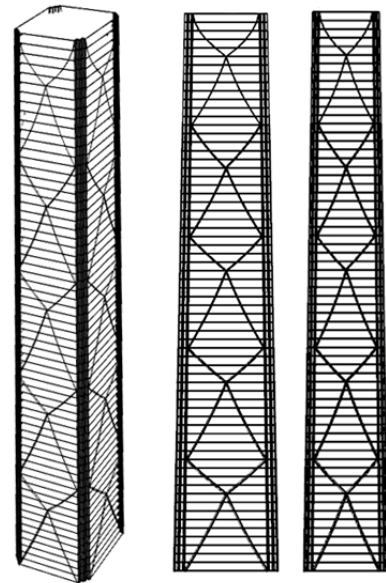
Figure 1. Various views of an optimal distributed bracing for a five section tower.

The computation of the lengths $l_i$ and inner forces $f_i$ is here processed with graphic statics. Graphic Statics is a theory and a set of methods that was first developed in [10] and [11]. It builds on two diagrams. The form diagram (length units) is the geometry of the reticulated network in equilibrium. The force diagram (force units) is a vectorial representation of the forces acting in the network. A rectilinear member in the form diagram has a corresponding parallel member in the force diagram with a length equal to the axial force magnitude in it. A node in the form diagram is in static equilibrium if the corresponding forces of its adjacent members form a closed polygon in the force diagram.

Graphic statics was first developed for structural analysis purposes and its use declined together with the advent of modern numerical solving methods. In the recent years, there has been a renewed interest in graphic statics for its benefits regarding the explorative shaping of structural equilibria [12][13][14]. In this paper, a procedural construction to build cable-like systems in equilibrium is developed thanks to graphic statics.
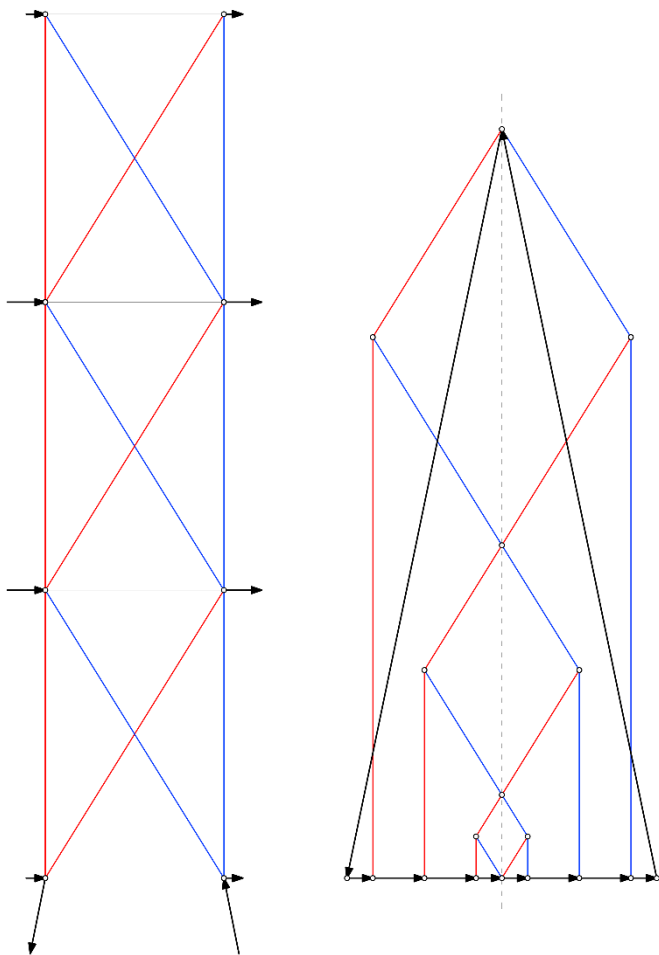


Figure 2. Form and force diagrams of conventional X-bracing. Horizontal loads are all applied on the left-hand side of the tower. It is assumed that half of them are transferred through the horizontal diaphragms to the right-hand side, which explains the symmetry.

The paper first reviews two existing discrete bracing typologies for tall buildings. A new bracing system that is optimal for distributed loads is then introduced and its procedural construction is explained. A comparison of the various systems is eventually drawn.

Figure 3.

II. REGULAR AND OPTIMAL DISCRETE BRACING SYSTEMS

The simplest lateral bracing system is the symmetric X-braced frame (Figure 2). The X-bracing sends the lateral loads upwards through the (moment resisting) corner column to the first bracing elements it meets, which respectively sends the lateral forces through shear to the following braces. This bracing system gained fame after the construction of the John Hancock Center designed by the architect Bruce Graham and the engineer Fazlur Kahn in Chicago in 1969.

An improvement one can further implement on the X-brace is to find the optimal (symmetric) intersection point that results in the least volume bracing. The solution for this problem is covered in [15] (Figure 4). For a cantilevered design space with a top point load to be braced with an X-frame, the optimum topology orientation consists of moving the central node from half the distance of the cantilever height (conventional X-brace) to 3/4 of that height.
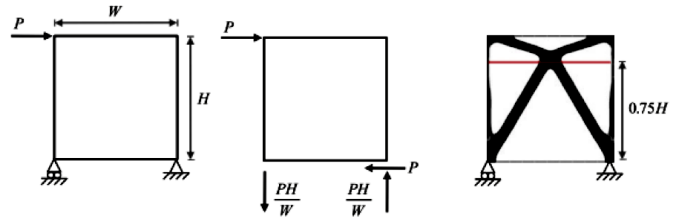


Figure 4. Cross-bracing with point load: (left) problem statement; (center) free body diagram; (right) topology optimization result. After [15].
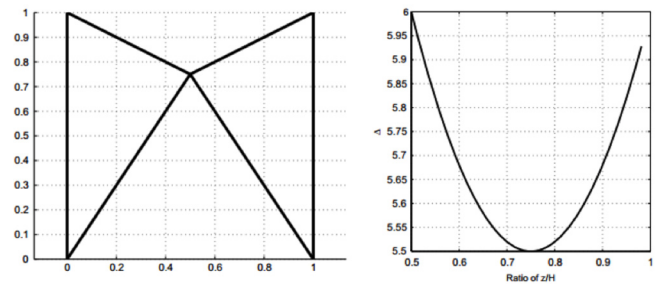


Figure 5. (left) Optimal linear cross-bracing. (right) deflection for various z/H ratios. After [15].

As seen in Figure 4, this results in an X-brace with longer members on the bottom and shorter members on top. Figure 5 again shows the optimum result of 0.75H in (a) but also shows a plot of the deflection of the member versus the ratio of z to H in (b), where z is the height of the central node.

Assuming that the solution z/h=0.5 (Figure 2) has a normalized strain energy of 1, the solution z/h=0.75 [15] has a normalized strain energy of 0.93, resulting in 7% of total volumetric savings compared to the X-brace baseline.

With the same geometric constraints and conditions of Figure 2, the force and form diagrams for the optimal bracing developed in [15] are seen on Figure 6.
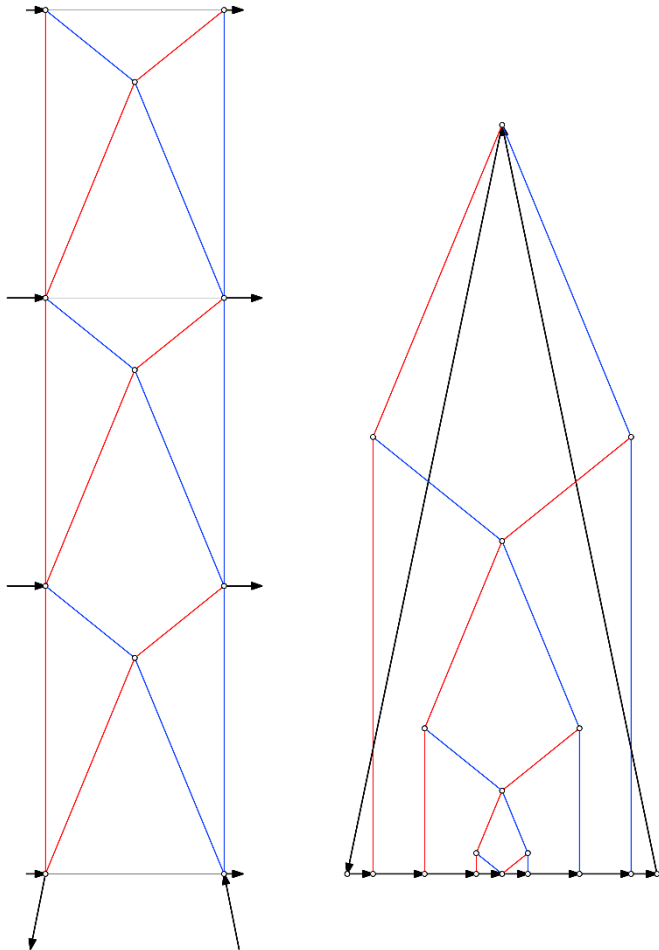


Figure 6. Form and force diagrams of the optimal bracing developed in [15]. Half the loads applied on the left side are assumed to be transferred to the right side through horizontal diaphragms.

This is indeed the optimal solution for the discrete problem. Nevertheless, tweaking some initial assumptions to achieve shorter load paths can result in significantly more efficient bracing designs, such as the following proposal.

## III. OPTIMAL DISTRIBUTED BRACING SYSTEM FOR ONE MODULE

While the optimal cross-bracing topology has already been determined, it depends on the key assumption that all of the lateral loads are transferred through one specific point on the corner columns as seen in Figure 7 (left). In a traditional tall building, all the lateral loads at each floor are distributed up to this point by the core and the corner columns which carry the

forces through shear. While this design is certainly sufficient, a lateral load travels first to the core and the corner columns up to the closest bracing intersection and finally down the bracing. This load path is clearly not the shortest one. Instead a better solution would be to find the form of the optimal bracing to carry the distributed lateral loads straight down the bracing from each floor slab and into the corner columns as seen in Figure 7 (right).
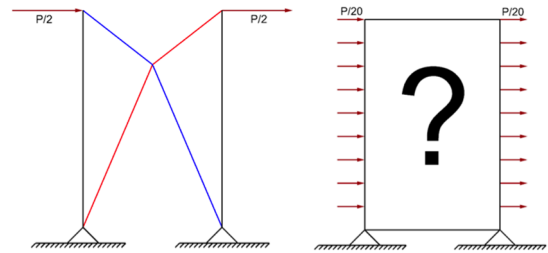


Figure 7. (left) Optimized bracing for lateral loading as a point load and (right) problem statement for optimizaed bracing for lateral distributed load.

When looking at the distributed load case in Figure 8 (a), the sections behave roughly the same as cross-bracing in the sense that the top-left and bottom-right sections are in compression (blue) and the other two sections are in tension (red). Assuming that half the distributed lateral load applied on the left side is transferred to the right side through the slabs, the bracing should be symmetrical with respect to the vertical axis. Also, the loading is anti-symmetric with respect to the same vertical axis. Therefore, elements in tension on one side of the axis are expected to be in compression on the other side. Thus, by symmetry this problem can be reduced into finding the optimal quadrant of the bracing as in Figure 8 (b). Finally, with the assumption that floor slabs or perimeter beams transfer the lateral loads to the bracing at each floor, the problem statement in Figure 8 (b) changes to that seen in Figure 8 (c). The lateral loads are now given as the floor-to-floor height multiplied by the building length and lateral load pressure.
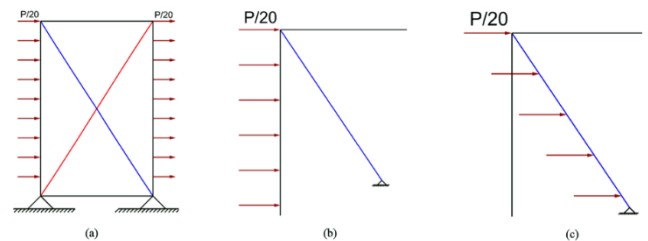


Figure 8. Distributed load case problem statement in (a) full scale, (b) quadrant section, and (c) lateral distributed load on the quadrant bracing.

For the problem statement of the lateral distributed loads on the quadrant (Figure 8, c), the optimal least-volume shape of the continuous bracing is simply that of a funicular arch. Using a graphic statics diagram with a horizontal load line as seen in Figure 9, the optimal bracing shape for purely axial compression forces becomes a funicular arch. This arch is dependent on the magnitude of the loading as well as the location of the central support, which is the only value that the optimization process has to obtain. Using this approach, then, the ideal arch can be mirrored vertically to produce the first quadrant (top left) of the bracing, and an identical process can be performed to form-find the remaining quadrants of the bracing (Figure 10).

It is worth noting that no connecting element is required between the bracing cross sections, resulting in large clear spans on the building.
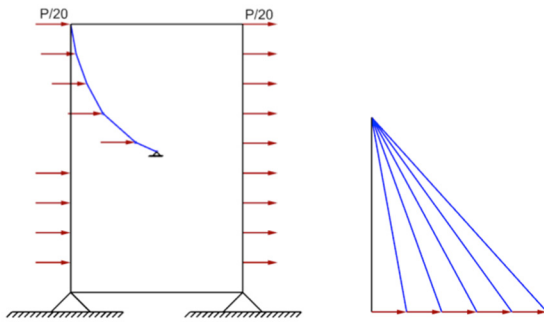


Figure 9. Form (left) and force (right) diagrams of optimal quadrant bracing shape for distributed load case.
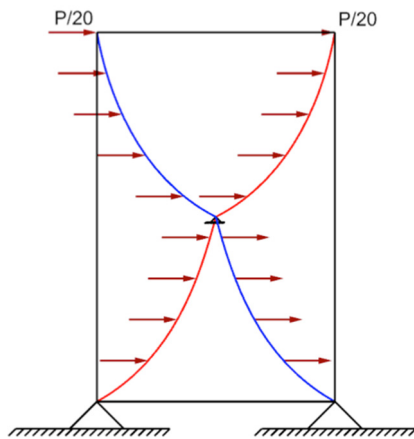


Figure 10. The distributed bracing for one section.

## IV. OPTIMAL DISTRIBUTED BRACING SYSTEM FOR MULTIPLE MODULES

Figure 11 shows the resulting geometry for the full tower over three sections. The geometric conditions are the same as in Figure 2 and Figure 4.

The minimum static action configuration for the full tower is the result of a process that is similar to the one described in the previous section. The number of variables is equal to the number of bracing modules. In the example Figure 12, two modules are considered and the Y position of points 4 and 8 are the only two parameters to be optimized. Figure 11 includes the optimal floor location for the center points.

Assuming those two parameters are given, one can construct the geometry of the entire bracing system in a procedural fashion. Figure 12 shows the process while using graphic statics diagrams.

The first quadrant is first considered (Figure 12, I). The point loads running from nodes 2 to 3 (form diagram) connect nodes a and b in the force diagram. In the form diagram, these four forces will be in equilibrium with two reactions applied on 2 and 3. The reaction on 2 is equal to $3/7^{th}$ of the resultant of the four forces. In the force diagram, a vertical line is drawn at a distance from a that is equal to $3/7^{th}$ of the distance a-b.
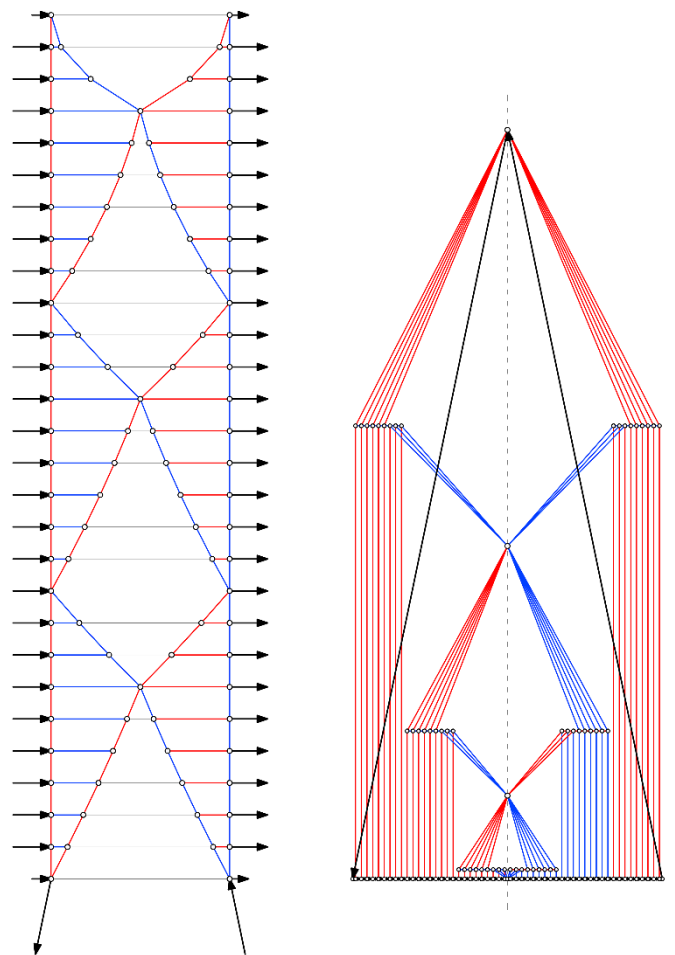


Figure 11. Form and force diagrams of the distributed bracing. Half the loads applied on the left side are assumed to be transferred to the right side through horizontal diaphragms.

Point c is then found at the intersection of that vertical line with an oblique line from a that is parallel to line 2-4. This point c provides the height of the radial lines introduced on Figure 9 and constructed on Figure 12, II.

The loads applied between nodes 3 and 5 (Figure 12, II) are then copied between nodes b and d in the force diagram. These loads would be in equilibrium with two reactions of equal magnitudes if these reactions were to be applied on nodes 3 and 5. Node e is consequently found at mid-distance between b and d. Node f is at the intersection of a vertical line running from e with a horizontal line running from c. Point g is at the intersection of the vertical axis of symmetry and a line from f that is parallel to the line 4-5. The radial lines can then be constructed in the force diagram (Figure 12, III) and their orientation can be copied in the form diagram between nodes 3 and 5.

Figure 12, III develops the lines needed to obtain node k similarly to Figure 12, I. Figure 12, IV develops the lines needed to obtain node q similarly to Figure 12, II. Figure 12, V completes the radial lines for the left hand side of the bracing system and Figure 12, VI mirrors it in order to finally describe the full bracing system.
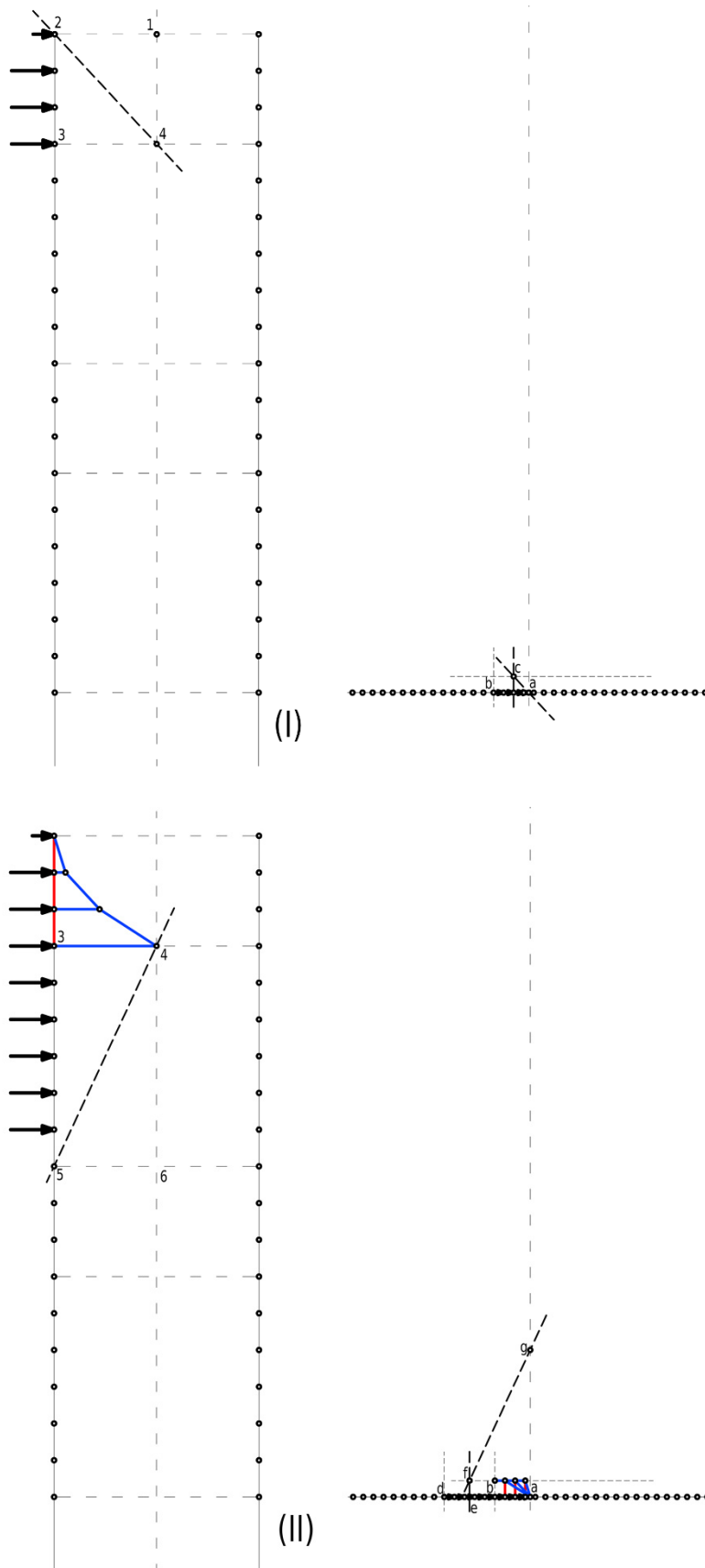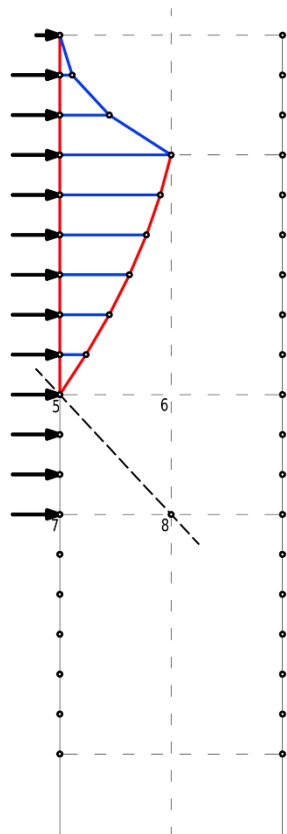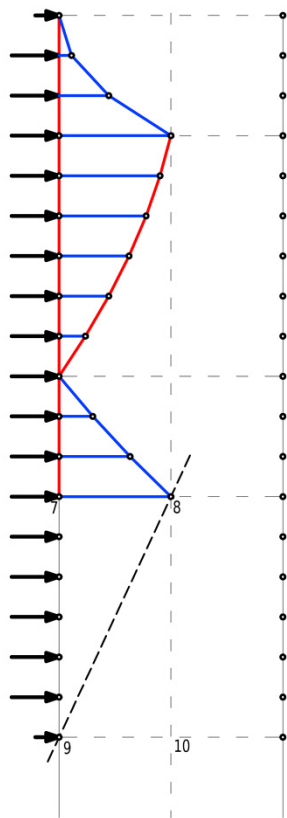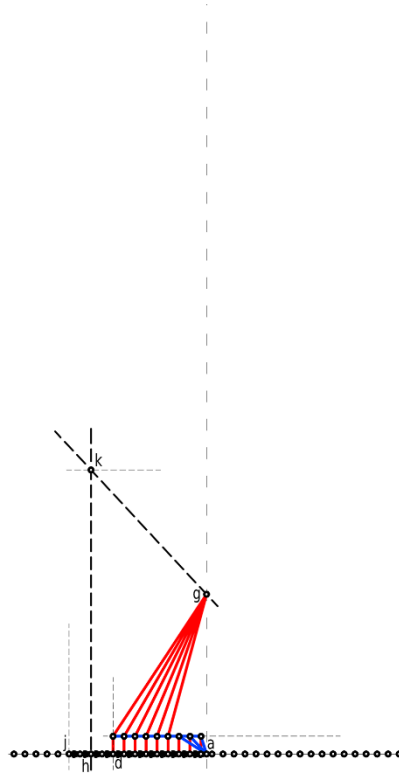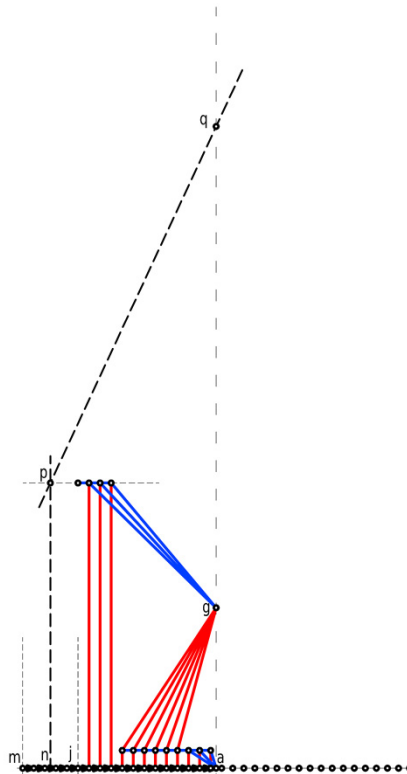
(I)

(II)

Figure 12. Procedural construction of the distributed bracing system, assuming the positions of intersection nodes 4 and 8 are given.

(III)



(IV)
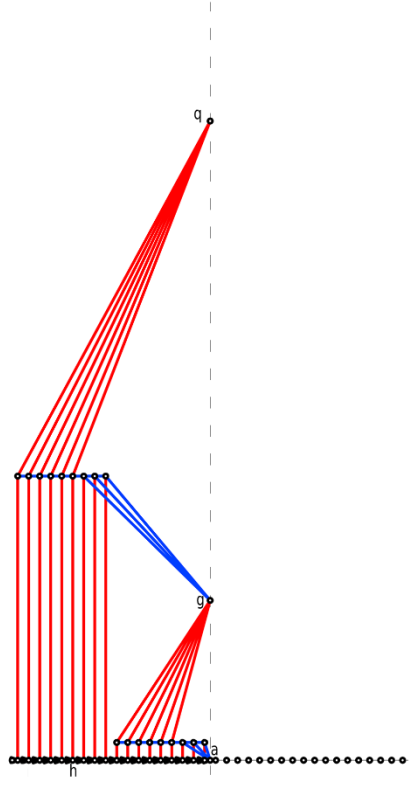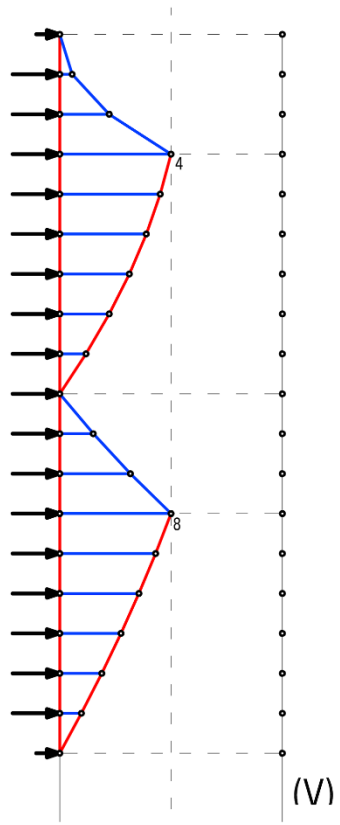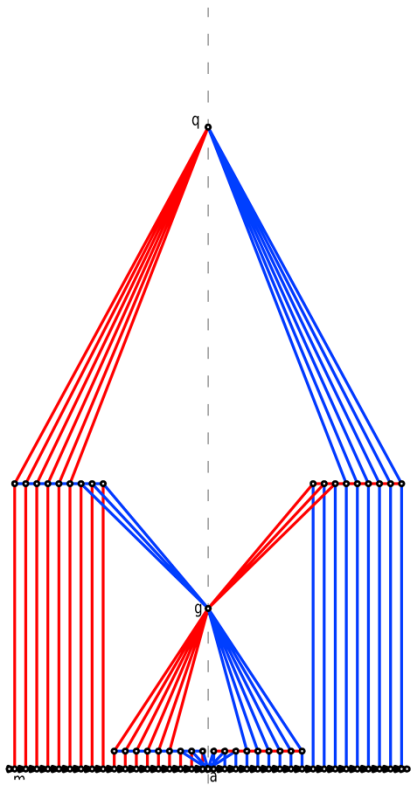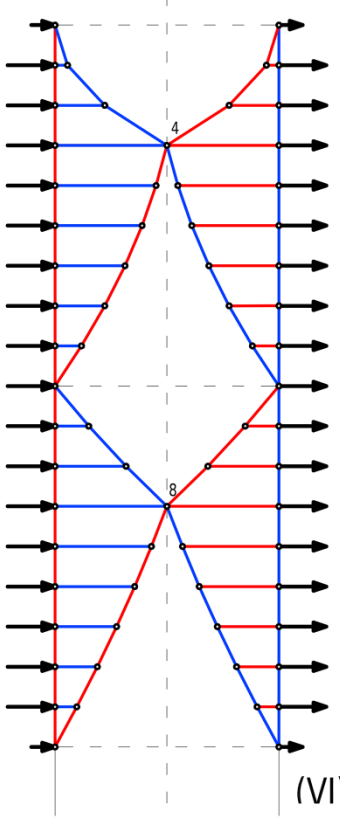
(V)

(VI)‴

## V. COMPARISON WITH PREVIOUS BRACING SYSTEMS

The corresponding strain energy of the proposed distributed bracing compared to that of the standard X-bracing and the optimal discrete bracing introduced in [15] can be seen in Table 1. For a single section of bracing, the distributed bracing saves over 50% of the strain energy compared to standard cross-bracing and more than 45% when compared to the bracing of [15]. Furthermore, while the two first bracing systems require a very stiff core to carry the shear loads up to the tips of the bracing, the suggested shape allows the loads to be transmitted directly from the perimeter beam or the floor slabs down through the bracing lines, instead of up to the bracing tips.

TABLE I.    PERFORMANCE OF SAVINGS FOR DIFFERENTS TYPES OF BRACING

| Type of Bracing | Strain Energy Factor | Volume Savings |
|---|---|---|
| X-Bracing | 1.00 | 0% |
| Optimal Discrete Bracing | 0.930 | 7.0% |
| Optimal Distributed Bracing | 0.464 | 53.6% |

While the energy and volumetric savings for the suggested bracing are very high for a single section, their efficiency decreases slightly as shear loads begin to dominate the distributed wind loads. As such, the top sections are much more efficient in their lateral design than the bottom sections (Table 2).

TABLE II.    SAVINGS PERFORMANCE FOR THE SUGGESTED BRACING RELATIVELY TO THE BRACING IN [15].

| Section Number | Volume Savings |
|---|---|
| **5** (53−65) | 53% |
| **4** (40−52) | 20% |
| **3** (27−39) | 10% |
| **2** (14−26) | 5% |
| **1** (0−13) | 3% |

Figure 1 shows the shape for a five section 800ft. (65 floor). Standard ASCE code assumptions where used for loading conditions and magnitudes. Despite its drop in efficiency over the height, it is clear that the suggested bracing is still significantly more efficient than both standard X-bracing and optimal discrete bracing from [15]. In the specific geometry of Figure 1, the full bracing of the tower still boasts a 24.6% and 17.9% volumetric savings over standard X-bracing and bracing of [15], respectively.

As the sections of the bracing progress down the building, their shapes vary slightly in order to guarantee equilibrium. As the bracings carry the shear load of the building down from section to section, the shear load carried from the above bracing becomes larger and larger compared to the distributed lateral load, as shown in Figure 13.
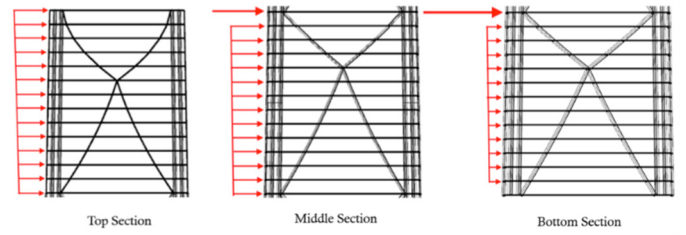


Figure 13. The form of the optimal discrete bracing changes as the building progresses from top to bottom.

If the building has no additional shear load transfer system away from the bracings, the loads will travel from the top bracing all the way through each section to the ground. Hence, the shear loading at the top of the section increases on the bottom sections respectively. Hence, the distributed wind load becomes negligible in the design of the bottom bracings as the magnitude of the shear load is of higher order.

As seen in Figure 13, the shear transfer of the building also has a significant effect on the shape of the bracing. Because the middle and bottom sections have a large point load on the top of the bracing from the shear of above sections, their shapes begin to approach that of the bracing from [15], where the shape is governed by the large point load on the top of the section.. Additionally, in reality the lateral loads (wind, earthquake) decrease proportionally to the height of the building, and thus the bottom sections handle not only a large shear load from the above sections but also a significantly smaller distributed lateral load.

## VI. DISCUSSION

This innovative and original shape both operates more optimally as well as provides a unique aesthetic shape and appeal. However the solution also implies the creation of a series of new construction challenges.

For instance, the shape of the bracing system is completely dependent on both the magnitude of the loading and the geometry of the building face. In order to maintain the integrity of the bracing behavior under different load cases, it is important that the bracing also resists in bending.

Additionally, wind loads applied on the face of the tower are assumed to be transferred through the slabs to the bracing. Yet, the connection between the slabs and the bracing can only transfer horizontal loads since it is not expected that the weight of the slabs is supported by the bracing. Lightweight connections must consequently be properly designed in order to ensure the viability of the full bracing system. Besides, the result provides a reasonable and replicable system from a manufacturing standpoint.

## VII. CONCLUSION

This paper introduced a new bracing typology for tall buildings that is of minimal static action. Assuming specific sizing and design approximations, this minimal static action criteria is similar to minimal volume or to minimal strain energy criteria.

The suggested bracing system is particular in the sense that it braces lateral loads at each single slab of the tall building. This feature results in a system that is not rectilinear but follows funicular curves.

A comparison with previous typologies addressing the same problem shows that the suggested bracing saves 18% of material volume when applied to a typical 800ft tower.

While an unconventional and unique lateral system, the bracing adds both a novel aesthetic appeal as well as an incredibly efficient system. These two considerations alone make it a promising choice as a lateral system for tall buildings, where lateral loads are a primary consideration in the structural design.

## REFERENCES

[1] A.R. Mijar, C.C. Swan, J.S. Arora, I. Kosaka, "Continuum topology optimization for concept design of frame bracing systems". J Struct Eng, ASCE 1998,124(5), pp. 541–50.

[2] Q.Q. Liang, Y.M.Xie, G.P. Steven, "Optimal Topology Design of Bracing Ssytems for Multistory steel Frames", J. Struct. Eng., 126(7), 2000, pp. 823-829.

[3] R. Baldock, K. Shea, "Structural Topology Optimization of Braced Steel Frameworks Using Genetic Programming". Intelligent Computing in Engineering and Architecture. Lecture Notes in Computer Science, vol 4200. Springer, Berlin, Heidelberg. 2006.

[4] W.F. Baker. "Energy-based design of lateral systems". Struct Eng Int 1992;2, pp. 99–102.

[5] M.M. Neves, H. Rodrigues, J.M. Guedes, "Generalized topology design of structures with a buckling load criterion", Struct Multidisc Optim 1995;10(2). pp. 71–78.

[6] Q.Q Liang. "Effects of continuum design domains on optimal bracing systems for multistory steel building frameworks". Proc 5th Australas Congr Appl Mech; vol. 2. Engineers Australia; 2007. pp. 794–799.

[7] S. Musmeci, La Statica e le Strutture, 1971, pp. 18-19.

[8] W.F. Baker, L.L. Beghini, A. Mazurek, J. Carrion, A. Beghini, "Structural Innovation: Combining Classic Theories with New Technologies", Engineering Journal, Third Quarter, 2015, pp. 203-217.

[9] T.Vanderbergh, W.P. De Wilde, "A review on conceptual design with morphological indicators", Int. J. Structural Engineering, Vol. 1, Nos. 3/4, 2010.

[10] W.J.M. Rankine, A manual of applied mechanics, London: R.Griffin, 1858.

[11] J.C. Maxwell, "On Reciprocal Figures and Diagrams of Forces", Philosophical Magazine, 27, 4, 1864, pp.250-261.

[12] W. Zalewski, E. Allen, Shaping Structures, John Wiley & Sons, 1997.

[13] T. Van Mele, L. Lachauer, M. Rippmann, P. Block, "Geometry-Based understanding of structures", Journal of the international association for shell and spatial structures, vol. 53, #4, 2012, pp. 285-295.

[14] C. Fivet, D. Zastavni, "Constraint-Based Graphic Statics: New paradigms of computer-aided structural equilibrium design", Journal of the international association for shell and spatial structures, vol. 54, #4, 2013, pp.271-280.

[15] L.L. Stromberg, A. Beghini, W.F. Baker, G.H. Paulino, "Topology optimization for braced frames: Combining continuum and beam/column elements", Engineering Structures, Vol. 37 pp. 106-124, 2012.